

Band structure and superconductivity of PdD_x and PdH_x†

D. A. Papaconstantopoulos

*Naval Research Laboratory, Washington, D. C. 20375
and George Mason University, Fairfax, Virginia 22030*

B. M. Klein

Naval Research Laboratory, Washington, D. C. 20375

E. N. Economou

Department of Physics, University of Virginia, Charlottesville, Virginia 22901

L. L. Boyer

Naval Research Laboratory, Washington, D. C. 20375

(Received 26 May 1977)

A study of the electronic band structure of the palladium-hydrogen system was made using the augmented-plane-wave method. The calculations were performed self-consistently for two choices of the exchange parameters within the $X\alpha$ scheme. Spin-independent relativistic corrections were included explicitly. The results for the energy bands are compared with previous calculations. Our results are found to be in good agreement with photoemission measurements. The calculations of the superconducting properties of this system are studied as a function of hydrogen content, utilizing the theory of Gaspari and Gyorffy and neutron-scattering data. The results for the superconducting transition temperature T_c are in very good agreement with the measured values. An analysis of these results attributes the observed inverse isotope effect to the effective increase of the Pd-H force constant over the Pd-D force constant, due to enhanced anharmonicity of the H motion, as originally proposed by Ganguly.

I. INTRODUCTION

The palladium-hydrogen system has received considerable attention recently, mainly due to the occurrence of superconductivity.¹⁻⁵ In this paper we give the details of our band-structure calculations, on which we based the superconductivity results that we reported previously,⁶⁻⁸ and further results on the hydrogen-concentration dependence of the superconducting properties of this system.

In Sec. II we discuss the energy bands, considering that PdD and PdH are identical in the band-theory model, i.e., neglecting the small difference of the lattice constants, and possible anharmonic effects as discussed by Miller and Satterthwaite.⁴ Our band calculations, which were performed self-consistently for different choices of the exchange parameters and the muffin-tin sphere radii, are compared with previous calculations and experiment.

In Sec. III we present local densities of states, decomposed per angular-momentum component and per site, together with a discussion of the interpolation schemes used.

In Sec. IV we review the electron-phonon interaction theory of Gaspari and Gyorffy⁹ and our method of extending it to compounds.¹⁰ Results of calculations of the superconducting properties for stoichiometric PdD and PdH are reported, which explain the inverse isotope effect. In Sec.

V results for substoichiometric PdD and PdH are presented, which explain the hydrogen-concentration dependence of the superconducting transition temperature.

II. BAND STRUCTURE

Schirber and Morosin¹¹ have measured the lattice constants of the β phase of PdH_x and PdD_x for the concentration range $0.8 < x < 0.98$. Their extrapolated values for $x = 1.0$ are 4.090 and 4.084 Å for PdH and PdD, respectively. Due to this very small difference between the lattice constants, we regard the band structure of PdH and PdD as identical, to within the accuracy of energy-band calculations. The lattice parameter used in our calculations was that of PdH. We also ignore any effects of the phonons on the band structure because (a) such effects, like the anharmonicity proposed by Miller and Satterthwaite,⁴ cannot be incorporated in present-day band calculations, and (b) the model discussed in Secs. IV and V explains adequately the superconducting properties of the Pd-H system without invoking these effects.

The band structure of stoichiometric PdH(D)_{1.0} was calculated in the NaCl structure by the augmented-plane-wave (APW) method, using first the $X\alpha$ exchange parameters 0.702 (Ref. 12) for Pd and 0.777 (Ref. 13) for H(D). This value of exchange for hydrogen was suggested by Slater,¹³ as producing the correct total energy for the H₂ molecule. The muffin-

fin-tin sphere radii ($R_{Pd} = 2.3795$ a.u. and $R_H = 1.4850$ a.u.) were chosen so that the starting crystal potentials were equal at the point of contact of the spheres. The exchange parameter for the interstitial region was set equal to $\frac{2}{3}$. The calculations were done self-consistently within the muffin-tin approximation and included relativistic effects (except spin-orbit splitting).¹⁴ We will denote the first iteration of this calculation as NSC_A and the final iteration as SC_A. We will also report on another self-consistent calculation (to be referred to as NSC_B and SC_B) that we performed by changing the exchange parameter of the hydrogen site to the value 0.978 as given by Schwarz.¹⁵

It has been shown¹⁶⁻¹⁸ that muffin-tin corrections can shift the energy levels by as much as 30 mRy. Since, however, these shifts occur almost uniformly in the d bands and cause small changes in the bandwidths of the order of 5 mRy, we have not included such corrections. Using perturbation theory¹⁹ we estimated the spin-orbit splitting and found a change of about 5 mRy in the d bandwidth, which is also a negligible correction for the purpose of calculating the Fermi level E_F and the densities of states (DOS). We have also checked the sensitivity of the energy bands to the size of the APW spheres, by performing a calculation with equal radii. Such a choice of radii is unrealistic for PdH since the hydrogen sphere encloses about 1.5 electrons. However, it is interesting to note that such an extreme choice of radii does not effect the d bandwidths by more than 13 mRy.

Each iteration of the APW calculation was carried out for 32 k points in the fcc Brillouin zone, and convergence to better than 5 mRy for the energy eigenvalues was reached after five iterations. Earlier work on calcium²⁰ has shown that the 32 k -point mesh is sufficient to obtain convergence to within 4 mRy for the fcc structure. The final potential was used to calculate the energy eigenvalues and the electronic charges inside the APW spheres for 89 k points in the $\frac{1}{48}$ of the Brillouin zone. More details on the techniques used to perform the band-structure calculations are given in the Appendix.

Figure 1 shows the energy bands of PdH(D) (calculation SC_A) plotted in the usual way across standard symmetry directions in the fcc Brillouin zone. For comparison, Fig. 2 shows our energy bands of pure Pd computed with exactly the same procedure ($X\alpha$ exchange, etc.) as in the PdH calculation, and with lattice constant equal to 3.89 Å. Inspection of Figs. 1 and 2 reveals the following three important differences: (a) The Fermi level of PdH (D) has moved to higher energy and is above the dense region of the d bands, where it falls in Pd. Thus, PdH has a much lower density of states

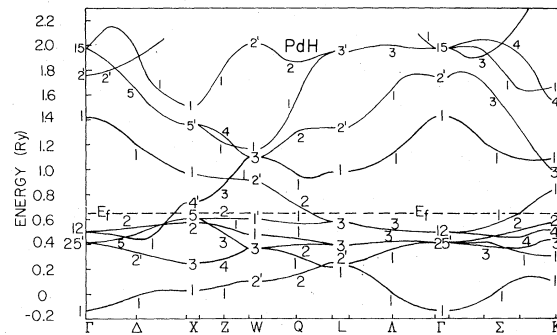


FIG. 1. Energy bands of PdH_{1.0}. Calculation SC_A.

at E_F than Pd; (b) the low-lying levels are bonding states; they are hybrids of s -like H with s - and d -like Pd states, lying about 2-eV deeper than the low s -like band of Pd metal; and (c) the anti-bonding states appear at about 3 eV above E_F for PdH.

We present in Table I a comparison of characteristic bandwidths for our results and those of Switendick²¹ and Zbasnik and Mahnig²² for PdH. The differences range from approximately 30 mRy for d bandwidths to over 100 mRy for the s - d separation. These differences indicate the combined effects of exchange, self-consistency and of including relativistic corrections. In order to compare the results of Table I we note that the calculation of Switendick²¹ is nonrelativistic (NR) and non-self-consistent (NSC) with full Slater exchange $\alpha = 1.0$; and that the calculation of Zbasnik and Mahnig²² (ZM) is also NR and NSC with exchange parameters $\alpha_{Pd} = 0.707$ and $\alpha_H = 1.0$. In comparing our calculation SC_A (see Table I) with that of Switendick we note good agreement in the s bandwidth, fair agreement in the d bandwidth and substantial disagreement in the s - d band separation. Comparing the calculation of ZM with our SC_A calculation we note small differences for the d bandwidths, but large differences for the rest of the widths. Our calculation NSC_B which was done with approximately the same exchange parameters as those of ZM

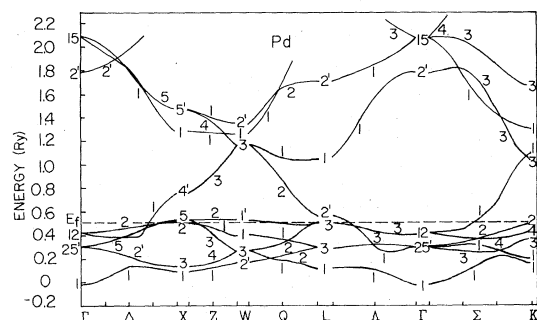


FIG. 2. Energy bands of Pd.

TABLE I. Comparison of energy separations of PdH expressed in Ry.

	Swit ^a	ZM ^b	NSC _A ^c	SC _A ^d	NSC _B ^e	SC _B ^f	NSER ^g	
X' ₄ -Γ ₁	0.868	0.997	0.880	0.867	0.953	0.922	0.871	s bandwidth
X ₅ -X ₃	0.307	0.353	0.328	0.333	0.323	0.332	0.313	d bandwidth
Γ ₁₂ -Γ' ₂₅	0.805	0.103	0.091	0.092	0.083	0.087	0.084	
Γ' ₂₅ -Γ ₁	0.423	0.631	0.538	0.546	0.632	0.627	0.541	s-d separation
Γ ₁ -Γ ₁	1.558	1.462	1.533	1.554	1.493	1.519	1.550	
X ₁ -X ₁	0.910	~0.98	0.929	0.936	0.944	0.950	0.904	s-band separation
L ₁ -L ₁	0.824	~0.85	0.746	0.754	0.734	0.744	0.754	

^aReference 21, $\alpha_H = \alpha_{Pd} = 1.0$.

^bReference 22, $\alpha_H = 1.0$, $\alpha_{Pd} = 0.707$.

^cPresent results, first iteration, $\alpha_H = 0.7772$, $\alpha_{Pd} = 0.702$.

^dPresent results, self-consistent, $\alpha_H = 0.7772$, $\alpha_{Pd} = 0.702$.

^ePresent results, first iteration, $\alpha_H = 0.978$, $\alpha_{Pd} = 0.702$.

^fPresent results, self-consistent, $\alpha_H = 0.978$, $\alpha_{Pd} = 0.702$.

^gPresent results, first iteration, equal radii, $\alpha_H = 0.7772$, $\alpha_{Pd} = 0.702$.

reveals that including relativistic corrections produces differences of the order of 30 mRy. Comparison of our NSC_A with SC_A and of NSC_B with SC_B calculations shows the effect of self-consistency. That is, we have negligible differences of the order of 5 mRy for the *d* bandwidths, but more substantial differences of the order of 20 mRy in some of the other characteristic widths. The effect of the exchange approximation on the bandwidths, seems to be more important than self-consistency. In summary, the *d* bandwidth is relatively insensitive to both exchange and self-consistency, but the other widths undergo changes exceeding 100 mRy in some cases. The last column of Table I displays results of our equal radii test. This calculation (NSER) was not self-consistent and was done with the same exchange parameters as NSC_A. A comparison between these two calculations shows that even for this rather unphysical choice of equal radii for PdH, the *d* bandwidths are changed by less than 10 mRy on the average. This test is an indication that muffin-tin corrections are not very important in this system.

Finally we report on the phenomenon of charge transfer, which we define by the quantity,

$$CT_s = 4\pi \int_0^{R_s} \Delta\rho_s r^2 dr,$$

where R_s is the radius of the muffin-tin sphere for a site s and $\Delta\rho_s$ is the difference between the final self-consistent charge density and the starting "superposed atomic" charge density (configuration $4d^{10}5s^0$, exchange of SC_A) within the muffin-tin spheres. We find that $CT_{Pd} = -0.291$ electrons and $CT_H = +0.125$ electrons. Therefore, we conclude that charge transfer occurs from Pd to H. Due to the muffin-tin constraint we cannot estimate the exact amount of charge transfer; it should

probably be no more than 0.3 electrons and no less than 0.1 electrons for reasonable values of R_s .

III. DENSITIES OF STATES

The 89 \vec{k} -point mesh eigenvalues $E_n(\vec{k})$ and the corresponding electronic charges within the APW spheres, were interpolated to 432 000 random \vec{k} points by Mueller's QUAD method,²³ to obtain the total DOS and also its angular-momentum components n_l inside the APW spheres. For the n_l 's we had to modify QUAD in order to perform the integration

$$n_l = \sum_n \int_s \frac{Q_{n,l}(\vec{k})}{|\nabla E_n(\vec{k})|} dS, \quad (3.1)$$

where $Q_{n,l}(\vec{k})$ are the electronic charges inside the muffin-tin spheres as defined by Mattheiss *et al.*²⁴

The DOS calculations following the above method were done for both the SC_A and SC_B PdH calculations and also for pure Pd. The rms fitting error for the energies was approximately 7 mRy for the sixth band and less than 4 mRy for the lower bands. As can be seen from Table I the essential difference between SC_A and SC_B is in the *s-d* separation. The low-lying bonding states of Fig. 1 (SC_A) are about 1 eV lower for the SC_B calculation. This is due to the fact that larger α_H means more attractive potential on H sites, thus states with large amplitude on H sites (*s* states) are lowered relative to those with small amplitude (metal *d* bands). However, the two different DOS's have very small differences near E_F . In what follows in the paper we will analyze our results on the basis of calculation SC_A, with some occasional references to calculation SC_B.

Figure 3 shows the total DOS of pure Pd and Fig. 4 that of PdH. From Fig. 3 we note that for Pd, E_F falls in a pronounced peak. To the contrary,

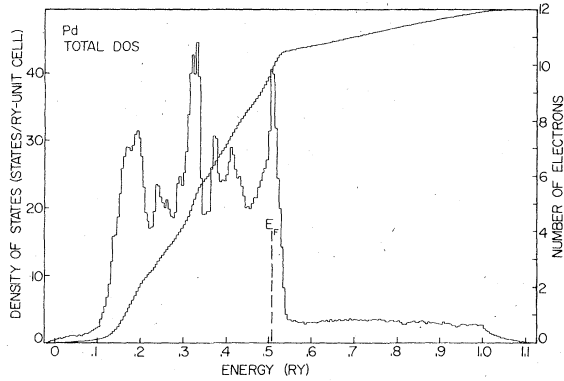


FIG. 3. Electronic density of states for Pd.

we observe from Fig. 4, which shows the total PdH DOS (calculation SC_A) and its *s*-like components for both the Pd and H(D) sites, a much lower value of DOS at E_F . Note that (a) the DOS of pure Pd

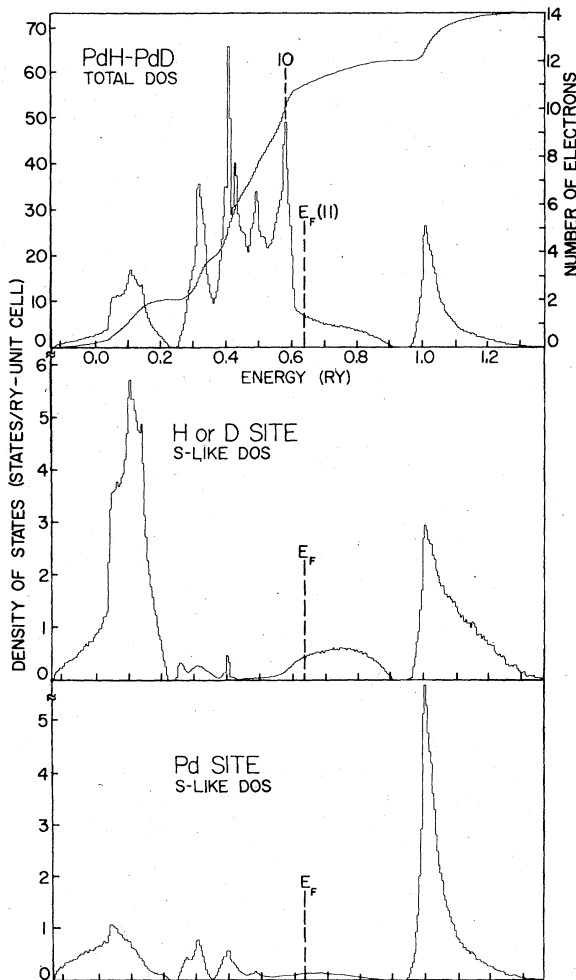


FIG. 4. Electronic densities of states for PdH_{1,0}. Top panel shows the total DOS and lower panels show the *s*-like DOS for H and Pd sites, respectively.

and of PdH above their high *d* peaks are quite similar; and (b) the total number of electrons below the highest *d* peak is the same (≈ 10) for Pd (Fig. 3) and PdH (Fig. 4), in spite of the significant differences in their DOS well below E_F . These observations can be utilized to justify the use of the rigid-band approximation (RBA) to estimate the Fermi level $E_F(x)$ for PdH(D)_{*x*}. One can write

$$10 + x = \int_0^{E_F(x)} n(E, x) dE \approx \int_0^{E_F(x)} n(E; 1) dE, \quad (3.2)$$

where $n(E; x)$ is the (DOS) for PdH(D)_{*x*}.

It is also interesting to observe that in the low-energy region (≈ 0.1 Ry) the H(D) site DOS is much higher than the Pd site DOS. By integrating the H *s* DOS, we find that a large fraction (about 0.5) of the H(D) *s* states participate in the formation of the low-lying hydrogen-palladium bonding states. These bonding states were observed by Eastman *et al.*²⁵ in photoemission experiments. Since these experiments were done on PdH_{0.6} we need to further interpret our calculations to compare with the measurements. To make this comparison, we will use the following arguments: An inspection of Figs. 1 and 2 shows that the low *s* band is lower in PdH than in Pd. Thus adding hydrogen to Pd lowers this band. The addition of H also raises E_F , pushing it above the *d* bands. Using Eq. (3.2) we estimate that for a hydrogen concentration of $x = 0.6$, E_F is equal to approximately 0.595 Ry. Also, from the positions of the peak of the *s* band for $x = 0.0$ (Pd) and $x = 1.0$ (PdH) we estimate (by linear interpolation) the position of the *s* band at $x = 0.6$ to be at approximately 0.17 Ry. Therefore, our band-structure results predict that these hydrogen-induced states are centered at 0.42 Ry, or 5.8 eV below the Fermi level, which is in good agreement with the measured value²⁵ of 5.4 eV. Such an agreement with the photoemission data can only be obtained from our calculation SC_A. Our calculation SC_B places the *s* band too low (approximately 1 eV), and this is why we base our analysis on SC_A.

Our assumption that the low *s* band shifts linearly with H concentration is consistent with the DOS results given by Zbasnik and Mahnig,²² who used the APW virtual-crystal approximation. A recent paper by Gelatt *et al.*²⁶ treats PdH_{*x*} in the average *t*-matrix approximation. These authors did not present DOS results and looking at their energy-band figures one cannot draw any definite conclusion as to the shifting of the *s* band with H concentration. On the other hand, Faulkner's²⁷ coherent-potential approximation (CPA) calculations indicate that the *s* band is not sensitive to hydrogen content. His results, however, are based on a rather inaccurate interpolation of our bands which probably leads to errors in his DOS. We be-

lieve that Faulkner's excellent theoretical development of the CPA for substoichiometric materials needs to be applied with a very accurate tight-binding Hamiltonian to answer the above questions.

The QUAD interpolation scheme may be criticized for not treating band crossings properly. We have checked this point with a Slater-Koster (SK) interpolation scheme which involves a 13×13 secular equation corresponding to s and p orbitals of Pd and H and the d orbitals of Pd. We have used 60 three-center energy integrals as parameters including up to fourth-nearest neighbors. The resulting total DOS at E_F is approximately 5% higher than that obtained by the QUAD approach. We have not utilized the SK partial DOS to calculate the electron-phonon interaction because we are not convinced that the SK scheme can yield these quantities (which depend on the wave functions) to a sufficient degree of accuracy. Faulkner²⁷ has developed the (CPA) formalism with a tight-binding Hamiltonian of the SK type. His results, however, are not in a form suitable to perform calculations of the electron-phonon interaction of the kind presented in Sec. IV. The reason is that the SK approach yields densities of states within the Wigner-Seitz cell, while the theory discussed in the next sections is formulated within the muffin-tin spheres. In addition, the SK scheme does not include the $l=3$ component of the DOS which is needed to perform these calculations.

IV. ELECTRON-PHONON INTERACTION AND T_c

According to the BCS theory, the superconducting state depends on Cooper pairing caused by the virtual exchange of phonons between electrons. The parameters which enter the theory of superconductivity and determine the transition temperature T_c are the electron-phonon coupling constant λ and the Coulomb pseudopotential μ^* .

Our calculation of the electron-phonon coupling constant λ was based on the theory of Gaspari and Gyorffy⁹ (GG) and on a generalization of McMillan's "constant- α " approximation.^{10,28} We have neglected the small nonspherical corrections to the GG formula discussed by Butler *et al.*²⁹ and by Gyorffy.³⁰

As was reported before,^{8,10} we have the following expressions:

$$\eta_j = n \langle I^2 \rangle_j$$

$$= \frac{E_F}{\pi^2 n} \sum_{l=0}^2 \frac{2(l+1) \sin^2(\delta_{l+1,j} - \delta_{l,j}) n_{l+1,j} n_{l,j}}{n_{l,j} n_{l+1,j}} \quad (4.1)$$

$$\alpha_j^2 = \eta_j / 2M_j \langle \omega_j \rangle, \quad (4.2)$$

$$\lambda_j = \eta_j / M_j \bar{\omega}_j^2, \quad (4.3)$$

$$\langle \omega^n \rangle_j = \int_0^\infty \omega^n F_j(\omega) d\omega, \quad (4.4)$$

$$\bar{\omega}^2 = \langle \omega \rangle_j / \langle 1/\omega \rangle_j, \quad (4.5)$$

$$\lambda = \sum_j \lambda_j. \quad (4.6)$$

The index j denotes an atom in the unit cell of atomic mass M_j , and $F_j(\omega)$ is the site-decomposed phonon DOS for atom j . In the present case $j=D(H)$ or Pd. Since $M_{Pd} \gg M_{H(D)}$, to a very good accuracy $F_{Pd}(\omega)$ and $F_{H(D)}(\omega)$ are the acoustical and optical mode parts of the phonon spectra, respectively.¹⁰

The phase shifts $\delta_{l,j}$, the DOS ratios $(n/n^{(1)})_{l,j}$, the total DOS n , the Fermi level E_F , and the electron-phonon interaction η_j were obtained from our band-structure calculations and are listed in Table II. The phonon spectrum $F_j(\omega)$ was taken from the analysis of neutron scattering data.³¹⁻³³ It should be mentioned that the phonon data were taken at $x=0.63$, while the $x=1$ phonon spectra are needed here. For the Pd part (which is essentially the acoustic part) we have estimated the $x=1$ spectrum by linearly extrapolating the experimentally determined acoustic spectra at³³ $x=0.0$ and $x=0.63$.^{31,32} This introduces a small decrease in $\langle \omega \rangle_{ac}$ of about 6% from its $x=0.63$ value. One can justify the linear extrapolation by observing that the change in ω_{ac} comes almost exclusively because of the slight linear increase in the lattice constant¹¹ with increasing x . The quantity $F_{D(H)}(\omega)$ varies with x both because the lattice constant changes with x and because the next-nearest neighbor environment is modified as x varies. These changes were estimated from the neutron scattering data,³¹ to be approximately 10% as x varies from zero to one and to be of opposite sign. Thus $F_{D(H)}(\omega)$ is expected to be almost x independent, and we have so treated it in our calculations.

It should be stressed that comparison of the experimental data on PdD_{0.63} and PdH_{0.63} reveals³² that the "harmonic" relation

$$F_H(\omega) = (M_H/M_D)^{1/2} F_D[\omega(M_H/M_D)^{1/2}] \quad (4.7)$$

is not satisfied. Actually it turns out that the ratio

$$M_H \langle \omega^2 \rangle_H / M_D \langle \omega^2 \rangle_D \approx 1.2, \quad (4.8)$$

instead of unity, which would hold in the harmonic case. In our calculations we have rescaled the optic mode density of states $F_D(\omega)$ of Rowe *et al.*³¹ to obtain

$$F_H(\omega) \approx 0.913 (M_H/M_D)^{1/2} F_D\{[0.913 (M_H/M_D)^{1/2} \omega]\}. \quad (4.9)$$

This rescaling satisfies the experimental observation that $M_H \langle \omega^2 \rangle_H = 1.2 M_D \langle \omega^2 \rangle_D$. Having obtained the various contributions to the phonon DOS we can

TABLE II. Quantities entering into the superconductivity calculations for PdD_{1,0} and PdH_{1,0}. Fermi level $E_F = 0.637$ Ry.

	Pd in PdD(H)	D(H) in PdD(H)	
	Densities of states [states/(Ry unit cell spin)]		
$n(E_F)$		3.301	
n_s	0.059	0.216	
n_p	0.137	0.040	
n_d	2.577	0.003	
n_f	0.008	0.002	
	Phase shifts		
δ_s	-0.415	1.075	
δ_p	-0.112	0.036	
δ_d	-0.394	0.001	
δ_f	0.003	0.000	
	Ratios $n_i/n_i^{(1)}$		
s	0.198	0.608	
p	0.420	0.456	
d	1.215	0.625	
f	0.677	13.190	
	Pd	D	H
$n(E_F)\langle I^2 \rangle$ (eV/Å ²)	0.865	0.392	0.392
$M\langle \omega^2 \rangle$ (eV/Å ²)	4.951	0.871	1.062
λ	0.175	0.450	0.369
μ^*		0.085	
T_c (calc) (°K)		9.6 (10.4) ^a	7.8 (9.0) ^a
T_c (meas) ^b (°K)		9.5-11.0	7.5-9.0

^aResults using the Allen-Dynes formula.

^bReferences 1-4.

write

$$[\alpha^2(\omega)F(\omega)]_{\text{PdH(D)}} = \begin{cases} \alpha_{\text{Pd}}^2 F_{\text{ac}}(\omega), & 0 \leq \omega \leq \omega_1, \\ \alpha_{\text{H(D)}}^2 F_{\text{opt}}(\omega), & \omega_2 \leq \omega \leq \infty, \end{cases} \quad (4.10)$$

with ω_j^2 given by Eq. (4.4) and ω_1 and ω_2 being the upper cutoff of $F_{\text{ac}}(\omega)$ and the lowest nonzero value of $F_{\text{opt}}(\omega)$, respectively.

Using the results in Eq. (4.10) we have calculated T_c by solving the linearized Eliashberg equations.³⁴ Our method of solution closely follows the formulation of Leavens³⁵ which we now summarize. Leavens shows that the equations

$$H_i = \sum_{j=0}^N [\lambda(i-j) + \lambda(i+j+1) - 2\mu_N^*] \frac{H_j}{G_j}, \quad (4.11)$$

$$G_j \equiv (2j+1) + \lambda(0) + 2 \sum_{j'=1}^j \lambda(j'), \quad j \geq 0, \quad (4.12)$$

$$\lambda(j) = 2 \int_0^\infty \frac{\omega \alpha^2(\omega) F(\omega) d\omega}{[\omega^2 + (2\pi k_B T_c)^2]} \quad (4.13)$$

must be satisfied with $H_0 = 1$, T_c being the transition temperature. Here μ_N^* is defined by³⁶

$$\frac{1}{\mu_N^*} = \frac{1}{\mu^*} + \ln\left(\frac{\bar{\omega}_2}{\omega_N}\right), \quad (4.14)$$

with

$$\bar{\omega}_2 = \left[\int_0^\infty \alpha^2 F(\omega) \omega d\omega / \left(\int \alpha^2 F(\omega) \frac{d\omega}{\omega} \right) \right]^{1/2}, \quad (4.15)$$

$$\omega_N = (2N+1)\pi k_B T_c,$$

and μ^* is the conventional Coulomb pseudopotential (see below).

The method of solution is to choose a starting set $\{H_i^{(0)}\}$ to generate via Eq. (4.11) sets of $\{H_i^{(1)}\}$ for several values of T_c . A value of $T_c^{(1)}$ is determined by interpolating using the condition $H_0^{(1)} = 1$. This procedure is continued until the solution converges, normally a few iterations, to obtain T_c to an accuracy of $\approx 0.1^\circ\text{K}$. The upper limit N is chosen so that the results are independent of N ; we find $N \geq 60$ is adequate for PdH(D)_x.

We have also obtained solutions for T_c using the Allen and Dynes³⁶ equation

$$T_c = \frac{f_1 f_2 \omega_{10g}}{1.2} \exp\left(-\frac{1.04(1+\lambda)}{\lambda - \mu^*(1+0.62\lambda)}\right), \quad (4.16)$$

$$f_1 = [1 + |\lambda/(2.46 + 9.35\mu^*)|^{3/2}]^{1/3}, \quad (4.17)$$

$$f_2 = 1 + \frac{(\bar{\omega}_2/\omega_{10g} - 1)\lambda^2}{\lambda^2 + (1.82 + 11.5\mu^{*2})\omega_2^2/\omega_{10g}^2}. \quad (4.18)$$

Here, $\bar{\omega}_2$ is defined in Eq. (4.15), and

$$\omega_{10g} \equiv \exp\left(\frac{2}{\lambda} \int_0^\infty \frac{d\omega}{\omega} \alpha^2 F(\omega) \ln \omega\right). \quad (4.19)$$

For details of how these equations were determined by Allen and Dynes we refer to Ref. 36. As discussed below, we find that solutions for T_c using Eq. (4.16) agree with the more exact Eliashberg solutions to within 10% for PdH(D).

We now proceed to discuss our results for $x=1$ which are listed in Table II. It should be mentioned here that these results are quantitatively different from those presented in Ref. 6. The reasons are twofold: (a) the main reason is that we have now used the APW results from an 89 \bar{k} -point mesh to generate the DOS, while we used a 20 \bar{k} -point mesh before. The new and more-accurate DOS values are $\sim 30\%$ lower at E_F than our earlier values and lead to the smaller values of λ . We have recently generated DOS from a 240 \bar{k} -point mesh for AgH and we find only a 3% deviation from the 89 \bar{k} -point mesh results. This assures us that at the 89 \bar{k} -point mesh we have reached adequate convergence; and (b) an additional smaller correction results from our now using the estimated phonon spectra at $x=1$ as described above and not the measured spectra corresponding to a H(D) concentration $x=0.63$. It is important to stress, however, that these new more accurate results do not change the physics of the situation; the ratio λ_D/λ_{Pd} is only slightly reduced from 3.4 to 3.1 with our new results. Therefore our previous explanation,^{6,7} which was first advanced by Ganguly,³⁷ that superconductivity in PdH(D) is mainly due to the interaction of electrons with the optic phonons (H vibrations) remains valid.

The results of Table II are based on our calculation SC_A, which gives the best agreement with photoemission data. We have also calculated the same quantities based on our results from SC_B. We find values for λ approximately 15% higher than the values of $\lambda_{PdD} = 0.62$ and $\lambda_{PdH} = 0.54$ reported here for SC_A. Switendick³⁸ predicted even higher values of λ , but he also found that the H(D) contribution is the dominant one.

The T_c values given in Table II were calculated with μ^* obtained from the following formula due to Bennemann and Garland,³⁹

$$\mu^* = 0.26n(E_F)/[1 + n(E_F)], \quad (4.20)$$

where here $n(E_F)$ is the total DOS at the Fermi level for both spins, expressed in units of states/eV unit cell spin.

We note that the Allen-Dynes T_c value is 0.8 °K (8%) higher than the Eliashberg solution value. Since such a difference in T_c would occur by changing either λ by $\sim 4\%$ or μ^* by $\sim 8\%$ we consider both solutions as being within the accuracy of the present calculations.

Our results for T_c in PdH and PdD are in excellent agreement with the observed values. Note especially that no adjustable parameters were used. In particular we have obtained a quantitative accounting of the observed inverse isotope effect. The physical origin of the isotope effect is the anharmonicity of the H(D) motion which produces an increase in $\langle \omega^2 \rangle_H$ by about 20% over the harmonic value $(M_D/M_H)\langle \omega^2 \rangle_D$; this increase makes $\lambda_D = 1.2\lambda_H$ and accounts quantitatively for the higher T_c in PdD. This mechanism as a possible explanation of the inverse isotope effect was first proposed by Ganguly³⁷; the present detailed calculations provide strong support for this idea.

V. SUPERCONDUCTIVITY OF SUBSTOICHIOMETRIC PdH(D)_x

In an earlier paper⁴⁰ we gave a summary of our calculations of T_c as a function of the hydrogen concentration x . We now present full details of these calculations.

Neglecting any clustering effects we assume that for $x < 1$ the PdH(D)_x system becomes a random one, because each H(D) site can be either occupied by H(D) with probability x or can be empty with probability $1-x$. To take this fact into account one must modify the basic equations (4.1)–(4.3) by taking a configurational average. Thus $\eta_j \rightarrow \langle \eta_j \rangle_{av}$, $\alpha_j^2 \rightarrow \langle \alpha_j^2 \rangle_{av}$, and $\lambda_j \rightarrow \langle \lambda_j \rangle_{av}$, where the symbol $\langle \rangle_{av}$ denotes configurational average. If j is a H(D) site, one can write

$$\begin{aligned} \langle \lambda_{H(D)} \rangle_{av} &= x \langle \lambda_{H(D)} \rangle_{av}^o + (1-x) \langle \lambda_{H(D)} \rangle_{av}^e \\ &= x \langle \lambda_{H(D)} \rangle_{av}^o, \end{aligned} \quad (5.1)$$

where $\langle \lambda_j \rangle_{av}^{(e)}$ is the average under the condition that the site is occupied (empty). The last step in Eq. (5.1) follows from the observation that an empty site does not contribute to the electron-phonon interaction. A similar expression was proposed by Gommersal and Gyorffy.⁴¹ We also have

$$\langle \alpha_{H(D)}^2 \rangle_{av} = x \langle \alpha_{H(D)}^2 \rangle_{av}^o, \quad \langle \eta_{H(D)} \rangle_{av} = x \langle \eta_{H(D)} \rangle_{av}^o. \quad (5.2)$$

In the present calculations we have omitted the variations in the phonon spectra with x . We have already argued above that this is a very good approximation for the optical part. For the acoustical

part one should expect an increase in $\langle\langle\omega\rangle_{\text{Pd}}\rangle_{\text{av}}$ of approximately 5% from the $x=1$ value as x varies in the range $0.70 \lesssim x \lesssim 1$, due to the decrease in the lattice constant. These changes in $\langle\langle\omega\rangle_{\text{Pd}}\rangle_{\text{av}}$ are expected to be largely compensated by the increase in η due to the contraction of the lattice. Since the latter have also been omitted, we expect our combined error to be of the order of 1%. Thus the problem has been reduced to the calculation of $\langle\eta_{\text{Pd}}\rangle_{\text{av}}$ and $\langle\eta_{\text{H(D)}}\rangle_{\text{av}}^0$. These two quantities depend on x both explicitly and implicitly through the x dependence of the Fermi level $E_F(x)$. We will make the further approximation of omitting the explicit x dependence of $\langle\eta_{\text{Pd}}\rangle_{\text{av}}$ and $\langle\eta_{\text{H(D)}}\rangle_{\text{av}}^0$. For the Pd site this approximation seems quite reasonable in view of the fact that the density of states for pure Pd ($x=0$) just above the highest d peak, where $E_F(x)$ lies, is quite similar to that of PdH(D) ($x=1$) as can be seen by inspection of Figs. 3 and 4. The fact that here we are interested in the much more limited range $0.7 \lesssim x < 1.0$, strengthens the validity of our approximation. An argument in support of omitting the explicit x dependence of $\langle\eta_{\text{H(D)}}\rangle_{\text{av}}^0$ is the following: as x varies in the range $0.7 \lesssim x \lesssim 1$ the immediate environment of an occupied H(D) site remains invariant, since it consists of Pd atoms; only the next-nearest neighbors will change because one creates some vacancies (their percentage does not exceed 30%). Hence the variation of $\langle\eta_{\text{H(D)}}\rangle_{\text{av}}$ with x is expected to be small. As a result of these approximations we can finally write

$$\langle\eta_{\text{Pd}}\rangle_{\text{av}} \approx \eta_{\text{Pd}}[E_F(x); x=1] \equiv \eta_{\text{Pd}}(x), \quad (5.3)$$

$$\langle\eta_{\text{H(D)}}\rangle_{\text{av}}^0 \approx \eta_{\text{H(D)}}[E_F(x); x=1] \equiv \eta_{\text{H(D)}}(x); \quad (5.4)$$

then we have

$$\langle\lambda_{\text{Pd}}\rangle_{\text{av}} \approx \eta_{\text{Pd}}(x)/M_{\text{Pd}}\bar{\omega}_{\text{Pd}}^2, \quad (5.5)$$

$$\langle\lambda_{\text{H(D)}}\rangle_{\text{av}} \approx x\eta_{\text{H(D)}}(x)/M_{\text{H(D)}}\bar{\omega}_{\text{H(D)}}^2;$$

TABLE III. Calculated and measured superconducting transition temperatures T_c (in °K); calculated electron-phonon mass-enhancement factors λ ; and Coulomb pseudopotentials μ^* as a function of hydrogen concentration x in PdD $_x$ and PdH $_x$.

x	μ^* ^c	λ_{tot}	$T_c(\text{calc})$	PdD $_x$		PdH $_x$			
				$T_c(\text{expt})^a$	$T_c(\text{expt})^b$	λ_{tot}	$T_c(\text{calc})$	$T_c(\text{expt})^a$	$T_c(\text{expt})^b$
1.00	0.085	0.62	9.6	9.8	10.3	0.54	7.9	8.0	9.1
0.96	0.087	0.56	6.6	7.8	9.1	0.49	5.2	6.3	6.6
0.92	0.091	0.52	4.9	6.4	7.1	0.46	3.6	4.8	4.8
0.89	0.093	0.49	3.5	5.0	5.1	0.43	2.5	3.5	3.1
0.85	0.093	0.44	2.1	3.7	3.3	0.39	1.4	2.2	2.1
0.81	0.097	0.41	1.4	2.5	...	0.37	0.9	1.3	...
0.77	0.101	0.36	0.6	0.33	0.3

^aReference 3.

^bReference 4.

^cEquation (4.20) in the text.

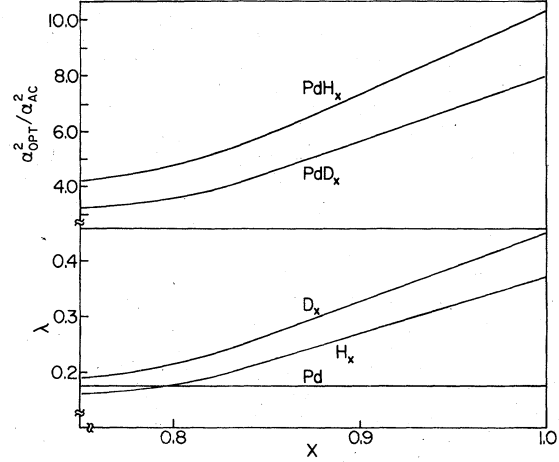


FIG. 5. Ratios of the optical to acoustical phonon-mode contributions to the tunneling spectrum (upper panel), and values of λ_j (lower panel) vs x in PdH $_x$ and PdD $_x$, respectively.

$$\langle\alpha_{\text{Pd}}^2\rangle_{\text{av}} \approx \eta_{\text{Pd}}(x)/2M_{\text{Pd}}\langle\omega_{\text{Pd}}\rangle, \quad (5.6)$$

$$\langle\alpha_{\text{D(H)}}^2\rangle_{\text{av}} \approx x\eta_{\text{H(D)}}(x)/2M_{\text{H(D)}}\langle\omega_{\text{H(D)}}\rangle.$$

Equations (5.3)–(5.6) together with Eqs. (3.1) and (4.1) solve completely the problem of determining T_c as a function of x in PdH $_x$, PdD $_x$.

It turns out (see Fig. 5) that the Pd-site contribution λ_{Pd} remains almost independent of x (for x in the range 0.7–1.0). On the other hand, $\lambda_{\text{H(D)}}$ shows a strong x dependence decreasing substantially with decreasing x . This decrease in $\lambda_{\text{H(D)}}$ is due mainly to a substantial decrease of $\eta_{\text{H(D)}}[E_F(x); x=1]$ with the lowering of the Fermi level $E_F(x)$. The physical origin of this effect can be understood from Fig. 4 where the H(D) site DOS is shown to decrease substantially as E_F is moving from the 11 mark ($x=1$) towards the 10 mark ($x=0$). The physical interpretation of this result is that

the nature of the electronic eigenstates at $E_F(x)$ is changing (with decreasing E_F) in such a way that the electrons spend less time around the H(D) site; consequently the electron-phonon interaction coming from the H(D) oscillations is reduced. The overall x factor in Eqs. (5.5) and (5.6) occurs because the appearance of vacancies with decreasing x further reduces the H(D) contribution to λ .

The ratio $\alpha_{op}^2/\alpha_{ac}^2$ is a strong function of x as shown in Fig. 5. This strong dependence may explain the discrepancies between the tunneling measurement of Dynes and Garno⁴² (who find that $\alpha_{op}^2/\alpha_{ac}^2$ is very large) and of Eichler *et al.*⁴³ (who find a value between 1 and 2). Anyway, our theoretical predictions shown in Fig. 5 and Table III can be checked by tunneling experiments in well-characterized samples.

In Table III we give our results for T_c versus x for both PdH_x and PdD_x together with the experimental data. The agreement is impressive especially in view of the fact that no adjustment of parameters was used. Note that the present theory predicts that the inverse isotope effect tends to disappear with decreasing x ; the reason is that this effect is due (according to the present analysis) to the optic contribution and as the latter is reduced the effect itself tends to go away.

According to the present theory the mechanism for increasing T_c with increasing x is as follows: by increasing x , the Fermi level $E_F(x)$ moves towards higher energies; at higher energies the s-like H(D) site component of the electronic eigenfunction is increasing substantially; this in turn produces most of the increase in λ and T_c . As can be seen in Fig. 4, this tendency continues beyond the value $x=1$ (mark 11). This probably explains why T_c can be as high as 16°K in certain palladium-noble metal hydrides.⁴⁴ The addition of Cu, Ag, or Au to PdH allows the Fermi level to move to even higher values than the 11 mark in Fig. 4, producing a further increase in the electron-phonon interaction and in T_c .

To further check the present theory, we have calculated [using our values for $n(E_F)$ and λ] the coefficient γ of the electronic specific heat and we have compared with the experimental data of Mackliet *et al.*⁴⁵ As can be seen from Table IV, the agreement is fairly good.

VI. SUMMARY

We have performed self-consistent APW band-structure calculations for PdH which are in good agreement with photoemission data. The densities of states and phase shifts resulting from these calculations have been used in conjunction

TABLE IV. Calculated and measured coefficient of electronic specific heat; calculated electron-phonon coupling constant λ ; and total density of states at the Fermi level $n(E_F)$, as a function of hydrogen concentration x .

x	λ	$n(E_F)$	γ_{calc}	γ_{expt}
			states/Ry unit cell spin	
			(mJ mole ⁻¹ deg ⁻²)	
1.0	0.54	3.30	1.77	...
0.96	0.49	3.42	1.77	...
0.92	0.46	3.64	1.84	...
0.89	0.44	3.77	1.88	1.53 ^a
0.85	0.39	3.76	1.81	1.56 ^a
0.81	0.37	4.02	1.91	1.50 ^a
0.77	0.33	4.32	1.99	...
0.73	0.26	6.28	2.75	...
0.0	0.47	15.10	7.69	9.40 ^b

^aReference 45.

^bReference 46.

with the theory of Gaspari and Gyorffy and neutron-scattering data, to study the superconducting properties of PdH_x and PdD_x. The results are in excellent agreement with experiment and show that T_c decreases with hydrogen concentration due to a rapid decrease of the average electron-phonon interaction associated with the H or D site. In addition, we verify the idea of Ganguly that the inverse isotope effect is due to the effective increase of the Pd-H force constant over the Pd-D force constant, due to enhanced anharmonicity of the H motion.

ACKNOWLEDGMENTS

We wish to thank M. M. Saffren for suggesting this investigation, J. S. Faulkner and A. C. Switendick for helpful discussions, L. S. Birks and D. J. Nagel for comments on the manuscript, and J. Sandelin for technical assistance. We are also indebted to J. M. Rowe for providing the phonon densities of states.

APPENDIX

The starting crystal potentials were generated by a superposition of relativistic atomic charge densities,⁴⁷ corresponding to the same exchange parameters used for the solid. A computer code for the construction of the starting and subsequent potentials of the self-consistency cycle is described in Ref. 48. The energy levels corresponding to the atomic 4s, 4p, 4d, and 5s states of Pd and the 1s state of H were all treated as bands. The inner levels of Pd were recalculated "atomiclike" in each iteration using appropriate modifications of the computer code of Ref. 47. Further details on

the performing of self-consistent calculations may be found in Refs. 20, 49, and 50.

The calculations were performed with the symmetrized version of the APW method.²⁴ The size

of the secular equation was chosen so that the criteria for convergence presented in Ref. 24 were satisfied. This resulted in a 90×90 matrix for the general points.

- †Work supported in part by NASA through subcontract Nos. 953918 and 954629 from the Jet Propulsion Laboratory at George Mason University; and by NSF Grant No. DMR 76-19458 at the University of Virginia.
- ¹T. Skoskiewicz, *Phys. Status Solidi A* **11**, K123 (1972).
- ²B. Stritzker and W. Buckel, *Z. Phys.* **257**, 1 (1972).
- ³J. E. Schirber and C. J. M. Northrup, Jr., *Phys. Rev. B* **10**, 3818 (1974).
- ⁴R. J. Miller and C. B. Satterthwaite, *Phys. Rev. Lett.* **34**, 144 (1975).
- ⁵D. S. McLachlan, T. B. Doyle, and J. P. Burger, *J. Low Temp. Phys.* **26**, 589 (1977).
- ⁶D. A. Papaconstantopoulos and B. M. Klein, *Phys. Rev. Lett.* **35**, 110 (1975).
- ⁷B. M. Klein and D. A. Papaconstantopoulos, in *Proceedings of the Fourteenth International Conference on Low Temperature Physics*, edited by M. Krusius and M. Vuorio (North-Holland, Amsterdam, 1975), Vol. 2, pp. 399-402.
- ⁸B. M. Klein, D. A. Papaconstantopoulos, and L. L. Boyer, in *Proceedings of the Second Rochester Conference on Superconductivity in d- and f-Band Metals*, edited by D. H. Douglass (Plenum, New York, 1976), pp. 339-359.
- ⁹G. D. Gaspari and B. L. Gyorffy, *Phys. Rev. Lett.* **29**, 801 (1972); R. Evans, G. D. Gaspari, and B. L. Gyorffy, *J. Phys. F* **3**, 39 (1973).
- ¹⁰B. M. Klein and D. A. Papaconstantopoulos, *J. Phys. F* **6**, 1135 (1976).
- ¹¹J. E. Schirber and B. Morosin, *Phys. Rev. B* **12**, 117 (1975).
- ¹²K. Schwarz, *Theor. Chim. Acta* **34**, 225 (1974).
- ¹³J. C. Slater, *Int. J. Quantum Chem. S* **7**, 533 (1973).
- ¹⁴L. F. Mattheiss, *Phys. Rev.* **151**, 450 (1966); J. O. Dimmock, *Solid State Phys.* **26**, 103 (1971).
- ¹⁵K. Schwarz, *Phys. Rev. B* **5**, 2466 (1972).
- ¹⁶P. D. DeCicco, *Phys. Rev.* **153**, 931 (1967).
- ¹⁷L. F. Mattheiss, *Phys. Rev. B* **5**, 290 (1972).
- ¹⁸D. D. Koelling, A. J. Freeman, and F. M. Mueller, *Phys. Rev. B* **1**, 1318 (1970).
- ¹⁹L. L. Boyer and B. M. Klein, *Int. J. Quantum Chem. S* **9**, 511 (1975).
- ²⁰J. W. McCaffrey, J. R. Anderson, and D. A. Papaconstantopoulos, *Phys. Rev. B* **7**, 674 (1973).
- ²¹A. C. Switendick, *Ber. Bunsenges. Phys. Chem.* **76**, 535 (1972).
- ²²J. Zbasnik and M. Mahnig, *Z. Phys. B* **23**, 15 (1976).
- ²³F. M. Mueller, J. W. Garland, M. H. Cohen, and K. H. Bennemann, *Ann. Phys. (N.Y.)* **67**, 19 (1971).
- ²⁴L. F. Mattheiss, J. H. Wood, and A. C. Switendick, *Methods Comput. Phys.* **8**, 63 (1968); **8**, 111 (1968).
- ²⁵D. E. Eastman, J. K. Cashion, and A. C. Switendick, *Phys. Rev. Lett.* **27**, 35 (1971).
- ²⁶C. D. Gelatt, J. A. Weiss, and H. Ehrenreich, *Solid State Commun.* **17**, 663 (1975).
- ²⁷J. S. Faulkner, *Phys. Rev. B* **13**, 2391 (1976).
- ²⁸W. L. McMillan, *Phys. Rev.* **167**, 331 (1968).
- ²⁹W. H. Butler, J. J. Olson, J. S. Faulkner, and B. L. Gyorffy, *Phys. Rev. B* **14**, 3823 (1976).
- ³⁰B. L. Gyorffy, in *Proceedings of the Second Rochester Conference on Superconductivity in d- and f-Band Metals*, edited by D. H. Douglass (Plenum, New York, 1976), pp. 29-57.
- ³¹J. M. Rowe, J. J. Rush, H. G. Smith, M. Mostoller, and H. E. Flotow, *Phys. Rev. Lett.* **33**, 1297 (1974).
- ³²A. Rahman, K. Skold, C. Pelizzari, and S. K. Sinha, *Phys. Rev. B* **14**, 3630 (1976).
- ³³A. P. Miiller, and B. N. Brockhouse, *Can. J. Phys.* **49**, 704 (1971).
- ³⁴G. M. Eliashberg, *Zh. Eksp. Teor. Fiz.* **39**, 966 (1960); **39**, 1437 (1960) [*Sov. Phys.-JETP* **11**, 696 (1960); **12**, 1000 (1961)].
- ³⁵C. R. Leavens, *Solid State Commun.* **15**, 1329 (1974).
- ³⁶P. B. Allen and R. C. Dynes, *Phys. Rev. B* **12**, 905 (1975).
- ³⁷B. N. Ganguly, *Z. Phys.* **265**, 433 (1973); *Z. Phys.* **B 22**, 127 (1975).
- ³⁸A. C. Switendick, *Bull. Am. Phys. Soc.* **20**, 420 (1975).
- ³⁹K. H. Bennemann and J. W. Garland, *AIP Conf. Proc.* **4**, 103 (1972).
- ⁴⁰B. M. Klein, E. N. Economou, and D. A. Papaconstantopoulos, *Phys. Rev. Lett.* **39**, 574 (1977).
- ⁴¹I. R. Gomersall and B. L. Gyorffy, *J. Phys. F* **4**, 1204 (1974).
- ⁴²R. C. Dynes and J. P. Garno, *Bull. Am. Phys. Soc.* **20**, 422 (1975).
- ⁴³A. Eichler, H. Wuhl, and B. Stritzker, *Solid State Commun.* **17**, 213 (1975).
- ⁴⁴B. Stritzker, *Z. Phys.* **268**, 261 (1974).
- ⁴⁵C. A. Mackintosh, D. J. Gillespie, and A. I. Schindler, *J. Phys. Chem. Solids* **37**, 379 (1976).
- ⁴⁶G. Choteau, R. Fourneaux, K. Gobrecht, and R. Tournier, *Phys. Rev. Lett.* **20**, 193 (1968).
- ⁴⁷D. A. Liberman, D. T. Cromer, and J. T. Waber, *Comput. Phys. Commun.* **2**, 107 (1971).
- ⁴⁸D. A. Papaconstantopoulos and W. R. Slaughter, *Comput. Phys. Commun.* **7**, 207 (1974); **13**, 225 (1977).
- ⁴⁹D. A. Papaconstantopoulos, J. R. Anderson, and J. W. McCaffrey, *Phys. Rev. B* **5**, 1214 (1972); J. R. Anderson, D. A. Papaconstantopoulos, J. W. McCaffrey, and J. E. Schirber, *ibid.* **7**, 5115 (1973).
- ⁵⁰J. W. D. Connolly, *Phys. Rev.* **159**, 415 (1967); S. Asano and J. Yamashita, *J. Phys. Soc. Jpn.* **30**, 667 (1971); P. Weinberger, K. Schwarz, and A. Neckel, *J. Phys. Chem. Solids* **32**, 2063 (1971).